



HAL
open science

Thermal generalist behaviour of invasive *Puccinia striiformis* f. sp. *tritici* strains under current and future climate conditions

Claude Pope de Vallavieille, B. Bahri, Marc Leconte, Olivier Zurfluh, Yosra Belaid, Essia Maghrebi, Frederic Huard, Laurent Huber, Marie Launay, Marie-Odile Bancal

► To cite this version:

Claude Pope de Vallavieille, B. Bahri, Marc Leconte, Olivier Zurfluh, Yosra Belaid, et al.. Thermal generalist behaviour of invasive *Puccinia striiformis* f. sp. *tritici* strains under current and future climate conditions. *Plant Pathology*, 2018, 67 (6), pp.1307-1320. 10.1111/ppa.12840 . hal-01811439

HAL Id: hal-01811439

<https://hal.science/hal-01811439v1>

Submitted on 8 Jun 2018

HAL is a multi-disciplinary open access archive for the deposit and dissemination of scientific research documents, whether they are published or not. The documents may come from teaching and research institutions in France or abroad, or from public or private research centers.

L'archive ouverte pluridisciplinaire **HAL**, est destinée au dépôt et à la diffusion de documents scientifiques de niveau recherche, publiés ou non, émanant des établissements d'enseignement et de recherche français ou étrangers, des laboratoires publics ou privés.



Distributed under a Creative Commons Attribution 4.0 International License

Thermal generalist behaviour of invasive *Puccinia striiformis* f. sp. *tritici* strains under current and future climate conditions

C. de Vallavieille-Pope^{a*}, B. Bahri^b, M. Leconte^a, O. Zurfluh^c, Y. Belaid^a, E. Maghrebi^a, F. Huard^d, L. Huber^c, M. Launay^d and M. O. Bancal^c

^aUMR BIOGER, INRA, AgroParisTech, Université Paris-Saclay, 78850 Thiverval-Grignon, France; ^bLaboratoire de Bio-agresseurs et protection intégrée en Agriculture, Institut National Agronomique de Tunis, Université de Carthage, 43 avenue Charles Nicolle 1082, Tunis-Mahrajène, Tunisia; ^cUMR ECOSYS, INRA, AgroParisTech, Université Paris-Saclay, 78850 Thiverval-Grignon, France; and ^dUS 1116 Agroclim, INRA, Domaine Saint Paul, Site Agroparc, 84914 Avignon Cedex 9, France

Yellow rust is a devastating wheat disease. Since 2000, *Puccinia striiformis* f. sp. *tritici* strains PstS1 and PstS2 have become adapted to high temperatures and have spread worldwide. By 2011, Warrior strains had invaded both warm and cold areas of Europe. This study questioned whether thermal aptitude promoted the spread of Warrior strains, similar to PstS1/PstS2, by comparing infection efficiency (IE) at five temperatures and latent period (LP) under warm and cold regimes for Warrior isolates and pre-2011 reference strains on two susceptible wheat varieties. The Warrior isolates showed a range of IE and LP responses to temperature that was intermediate between the northern reference isolates adapted to cold conditions and both the southern and invasive PstS2 isolates adapted to warm conditions. Warrior isolates had the highest IE under optimal temperatures of 10 and 15 °C, and displayed reduced infectivity under the warmest (20 °C) and coldest (5 °C) temperatures. Warrior strains acted as thermal generalists and the reference isolates acted as specialists. An IE thermal response was used to simulate the development of each isolate under future climate scenarios in a temperate and Mediterranean region. Isolates had the same ranking for yearly IE over the three 30-year periods (1971–2000, 2021–2050, 2071–2100) and both locations, with a slight infection increase in the future. However, in the future IEs increased in earlier months. The thermal generalist profile of Warrior isolates for IE was confirmed, with an intermediate capacity to tolerate warming climate, whereas the southern isolates are better adapted to warm conditions, but do not have the virulences necessary to develop on current varieties.

Keywords: climate change, latent period, modelling, thermal adaptation, *Triticum aestivum*, wheat yellow (stripe) rust

Introduction

Predicting future occurrence of plant diseases requires not only reliable climate change scenarios, but a characterization of the pathogen response to climate modifications (Garrett *et al.*, 2011; Sutherst *et al.*, 2011; Launay *et al.*, 2014). Such responses may involve spore migration, phenotypic plasticity and genetic adaptation to climate and climate change-driven shifts in ecosystem attributes. Recent pathogen population shifts have been well documented (Hovmøller *et al.*, 2016; Mariette *et al.*, 2016a; Schwessinger, 2016; Walter *et al.*, 2016). Climate change impact on pathogen biodiversity is often considered as a forcing variable that drives demographic response via species distribution, extension range, outbreaks (Bebber, 2015) and the genetic evolution of species. Moreover, predicting the impact of climate on future epidemics requires a better understanding of pathogen adaptation to changing climate (Garrett *et al.*, 2011). The response of plant–pathogen interactions to

temperature is largely nonlinear (Bernard *et al.*, 2013) and may be used to infer climate change impacts on pathogen aggressiveness. One approach to study plant pathogen response to temperature is to model pathogen strain adaptation rates in response to changing temperatures. However, experimental validation of this type of model is not available, given that monitoring pathogen physiological or genetic adaptation requires extensive laboratory measurements of fitness traits across diverse environmental conditions. Therefore, scientists must incorporate large uncertainty to climate change risk assessments to overcome lack of knowledge about processes of pathogen adaptation to temperature (Sutherst *et al.*, 2011). Another approach taken in the present study involves establishing the current thermal response of well-characterized strains previously adapted, or not, to high temperatures. In this case the thermal response curves can be used under future climate models to understand if local thermal adaptations observed today provide an advantage to the strains in a warmer climate. To the authors' knowledge, this approach is similar to the well-known temperature reaction norm in ecology

*E-mail: claude.pope-de-vallavieille@inra.fr

(Bernard *et al.*, 2013), but has been poorly used with a large range of isolates to predict future epidemic risks. This approach would help to determine whether current invasive strains that developed under warmer climates have a selective advantage at the end of the century. Wheat yellow (stripe) rust, caused by *Puccinia striiformis* f. sp. *tritici* (Pst), has previously shown preferential development in cold areas, but was recently able to invade warmer regions. Hence, it was identified as a good candidate disease to address the question of thermal adaptation. Indeed, new aggressive strains of Pst (PstS1 and PstS2) tolerant to high temperature have recently spread worldwide (Milus *et al.*, 2009; Walter *et al.*, 2016).

Yellow rust is a major disease of wheat (*Triticum aestivum*) in temperate areas with cool and wet summers and mild winters (Rapilly, 1979; Hovmöller *et al.*, 2011; Wellings, 2011; Ali *et al.*, 2014; Chen *et al.*, 2014). The deployment of resistant wheat varieties remains the most effective means to control yellow rust (Paillard *et al.*, 2012; Sørensen *et al.*, 2014). So far, more than 70 validated resistance genes, designated *Yr*, have been reported (<http://www.shigen.nig.ac.jp/wheat/komugi/>) and Pst pathological surveys have been conducted all over the world (Chen, 2005; Hovmöller *et al.*, 2011; de Vallavieille-Pope *et al.*, 2012; Ali *et al.*, 2014). High temperatures during the growing season have been considered a constraining factor for Pst development and its long-distance dissemination (Brown & Hovmöller, 2002). Despite this selective pressure and in the context of global climate change, many worldwide major epidemics occurred between 1999 and 2002 in the south-central United States (Milus *et al.*, 2006, 2009) and Australia (Wellings, 2011; Loladze *et al.*, 2014). An incursion of a new aggressive strain, PstS1, at higher temperature occurred in regions previously considered too warm for the development of wheat yellow rust. Furthermore, this incursion was observed in North Africa (Bahri *et al.*, 2009) and southern France in 2004, with a close lineage, PstS2. However, the epidemic did not progress due to effective *Yr* resistance genes in the commonly grown varieties (de Vallavieille-Pope *et al.*, 2012). As most yellow rust studies were based on molecular diversity and virulence phenotyping, it allowed a good appreciation of the broad characteristics of an international population. However, few studies addressed the effect of host-climate factors on infection components at the population level and only included one or a few isolates. So far, experiments estimating the latent period (time between inoculation and the first appearance of spores) and spore production have determined that strains PstS1/PstS2 from East Africa (Walter *et al.*, 2016) are more aggressive than the pre-2000 US Pst isolates at 18 °C (Milus *et al.*, 2009). This thermal adaptation and unprecedented increase in aggressiveness in populations of pathogenic fungi can be driven by phenotypic plasticity and genetic differentiation. The structure of the French Pst population before 2004 also demonstrated a local thermal adaptation: southern isolates persisted at high temperature under a

warmer Mediterranean climate, whilst northern isolates showed an infective superiority at lower temperatures (Mboup *et al.*, 2012). Besides a varietal effect, the effect of temperature on Pst aggressiveness components can be dramatic, as noticed recently with North American and Australian PstS1 isolates (Milus *et al.*, 2009; Loladze *et al.*, 2014). The race Warrior is another exotic strain invading new regions; it appeared in 2011 in northwestern Europe and rapidly replaced the European Pst population. This race was found in both warm and cold areas, from Sweden to Spain (Hovmöller *et al.*, 2016), suggesting its adaptation to a broad range of temperatures. However, temperature reaction norms of different Warrior strains have not been established yet.

In order to define a range of aggressiveness profiles with regards to temperature, under controlled climate conditions, this study compared the response to temperature of invasive Warrior isolates to reference Pst isolates: PstS2 (adapted to warm temperatures) and isolates from the north and south of France (adapted to cold and warm temperatures, respectively) (Mboup *et al.*, 2012). Infection efficiency and latent period were measured at a range of temperatures. Furthermore, this dataset was used to parameterize an infection model based on temperature for each isolate, and this model was used to simulate infection efficiency for each isolate in temperate and Mediterranean regions for near future (2021–2050) and far future (2071–2100) climate scenarios. The comparison between invasive Warrior strains and other reference isolates leads to generalist versus specialist behaviour analysis that considers infection efficiency and latent period responses to temperature.

Materials and methods

Pathogen isolates, pathotypes and genotypes

Sixteen Pst isolates, representative of the recent Warrior invasion, and reference isolates were selected for this study. Isolates are part of the National Institute for Agricultural Research (INRA Grignon, France) annual pathogen race survey collection (de Vallavieille-Pope *et al.*, 2012). The selected isolates were chosen on the basis of year, species (wheat or triticale (*×Triticosecale*) variety) and location, and included nine Warrior isolates (W1–W9) collected in France, with the exception of W8 which was collected in Spain (Table 1). The reference isolates included three isolates of PstS2 (P1 to P3) from southern France, Tunisia and Algeria, respectively; two northern French isolates adapted to cold temperature (N1 and N2) and two southern French isolates adapted to warm temperature (S1 and S2) (Mboup *et al.*, 2012). The N1, N2, S1 and S2 isolates were selected for their average behaviour in response to temperature (Mboup *et al.*, 2012). Furthermore, isolates P1–P3 were chosen according to their different geographic origins to represent the highest diversity possible. Fourteen isolates originated from bread wheat, and isolates W5 and W9 were collected from triticale. The isolates, originating from a single sporulating lesion, were stored at –80 °C and were purified from a single sporulating lesion before the current study, and genotyped and pathotyped. The Pst isolates were genotyped using 20 microsatellite markers (Ali *et al.*, 2011).

The virulence phenotypes of the Pst isolates were assessed using 32 wheat differential varieties, including 15 European and world differential varieties (Johnson *et al.*, 1972) and Kalyansona (Yr2), Federation × 4 Kavkaz (Yr9), Clement (Yr9, YrCle), VPM1 (Yr17), Rendez-Vous (Yr17+), TP981 (Yr25), Opata 85 (Yr27), Anza (YrA), Ambition (YrAmb), Sterling (YrSter), Warrior (YrWar) and the Australian isogenic lines Yr5, Yr6, Yr7, Yr8, Yr15, Yr24 in the Avocet near-isogenic lines background (see http://www.ars.usda.gov/SP2UserFiles/ad_hoc/36400500Resistancegenes/Yrgene.xls). Pathotyping is described in de Vallavieille-Pope *et al.* (2012). The isolate pathotypes and genotypes are described in Table 1.

Spore production

Prior to the study, spores of the Pst isolates were produced on the susceptible wheat variety Victo. Seedlings of Victo were grown to the two-leaf stage (about ten day-old) in pots filled with standard peat soil (blocking substrate type 5; Gebr. Brill Substrate GmbH & Co. KG) in an air-filtered chamber inside a greenhouse with 15 °C/8 h dark and 20 °C/16 h natural light. Considering that light duration and intensity affect infection efficiency (de Vallavieille-Pope *et al.*, 2012), this period was supplemented with an additional artificial light provided by sodium vapour lamps (light intensity: 150 $\mu\text{mol m}^{-2} \text{s}^{-1}$) the day before inoculation. Wheat seedlings 1 cm-high were growth-regulated with a maleic hydrazide solution (3,6-dihydroxypyridazine; Duchefa Biochemie B.V.) at a concentration of 0.25 g L⁻¹ and about 20 mL per pot in order to increase their yield by restricting growth to the primary seedling leaf. Spores stored at -80 °C were taken out of the freezer and immediately heat shocked at 40 °C for 10 min before use. Spores (3 mg) were suspended in 600 μL of engineered fluid (Novex 7100) for inoculation onto seedlings (Sørensen *et al.*, 2016). After incubation at 8 °C for 24 h in the dark in a dew chamber, plants were placed in an air-filtered chamber inside a greenhouse maintained at the same controlled conditions as above. To minimize pathotype cross-contamination, recently inoculated seedlings were placed in clear cellophane bags (Helmut Schmidt Verpackungsfolien GmbH). At 14–17 days post-inoculation (dpi), the bags were gently shaken to dislodge urediniospores into glass tubes. Collected urediniospores were dried in a desiccator at 4 °C for 3 days. The spore production was repeated three times under the same conditions and the third production was used in the study to homogenize spore physiological quality.

Plant material

Two wheat varieties, Victo and Cartago, known to be highly susceptible to Pst, were used for this study. Fifteen seeds of each variety were planted in square pots (7 × 7 × 8 cm) in the soil mix described above. Wheat seedlings were grown in greenhouse rooms under the same controlled conditions described above until the first seedling leaf was fully expanded, and the second leaf was partially exposed. The plants were not treated with maleic hydrazide in the temperature treatment experiments. Plants were thinned to 10 homogeneous plants per pot and second leaves were eliminated the same day as inoculation.

Infection efficiency assessment

Four pots of 10 wheat seedlings per pot of each variety (Victo and Cartago) were inoculated with 1 mg of urediniospores of each Pst isolate suspended in 1 mL Novex 7100, corresponding

to 110 spores cm⁻². After inoculation, 40 seedlings were placed at 100% RH in the dark for 24 h at one of the five post-inoculation temperatures (5, 10, 15, 20 and 23 °C). Then, the pots were transferred into a growth chamber set at 19 °C/16 h light period (light intensity: 350 $\mu\text{mol m}^{-2} \text{s}^{-1}$) and 8 h/14 °C dark period, considered as optimal conditions for Pst incubation. Because of its semisystemic development, Pst infection efficiency (IE) was estimated by counting the numbers of chlorotic spots approximately 7 dpi on a 4–5 cm² area in the middle of each leaf. The experiment, consisting of five post-inoculation temperatures during the dew period, was conducted twice. IE was assessed as the number of chlorotic spots per deposited urediniospore × 100.

Latent period assessment

Four pots of 10 wheat seedlings per pot of each variety (Victo and Cartago) was used for the latent period (LP) test for each temperature regime (cold and warm). Pathogen inoculum was prepared by mixing 1 mg of urediniospores from each Pst isolate with 25 mg of talcum powder. Inoculum was locally applied to the adaxial sides of leaves by gently pressing the edge of a plastic label (thickness *c.* 1 mm) onto the central part of the leaves to form a narrow band of spores across the leaf (Sørensen *et al.*, 2014).

After incubation in the dark at 10 °C for 24 h under dew conditions, plants were placed into two climatic chambers under warm and cold regimes. The warm regime (16/25 °C) comprised 25 °C for a 16 h-light period (intensity: 350 $\mu\text{mol m}^{-2} \text{s}^{-1}$) and 16 °C for a 8 h-dark period. For the cold regime (10/15 °C) the chamber was set at 15 °C for a 16 h-light period and 10 °C for a 8 h-dark period. This experiment was conducted twice.

The number of sporulating lesions was counted daily starting 8 dpi and stopping at 20 dpi. Latent period was assessed as the number of hours post-inoculation (hpi) to the appearance of Pst sporulating lesions on half of the seedlings (Milus *et al.*, 2006) using two methods. First, the evolution over time of the number of sporulating lesions on inoculated leaves was adjusted for each isolate, variety and temperature regime to a linear generalized logistic model, using all four replicates together. Confidence intervals at the 95% level were estimated by bootstrap analysis using 10 000 randomized data-pull events and LP was estimated as the inflexion points. Alternatively, LP was estimated for each replicate as the mean duration (in hours) from inoculation to sporulating lesion appearance per isolate, variety and temperature regime combination. Both estimations of LP were similar and the latter method was further used to identify significant differences among strains.

Data analysis

Analysis of variance (ANOVA) of IE and LP of the 16 Pst isolates was performed for each of three dew period temperatures (5, 10 and 15 °C; there was rare or no infection at dew period temperatures of 20 and 23 °C, respectively) and each of the two temperature regimes (cold (10/15 °C) and warm (16/25 °C)). The effects of host variety, pathogen isolate and temperature were investigated in factorial multiple analyses of variance (MANOVA). To meet the assumptions of homoscedasticity and normality, arcsin (square-root) transformation was used for IE. LP data were not transformed. For both IE and LP, the values of 10 seedlings per pot were averaged to obtain a mean IE and LP per combination of isolate, temperature and variety. Each pot represented a replicate that was used in MANOVAs.

ANOVAs were not performed for IE at 20 and 23 °C during the dew period because very few and no infections were observed, respectively, and thus the assumptions of homoscedasticity and normality were not met. In order to analyse the differences in IE between isolates at a temperature of 20 °C during the dew period, the probability of infection (P_i) of the 16 isolates (where 0 = no infection and 1 = infection) was compared for each variety separately using Newman–Keuls comparison at the 5% significance level. A principal component analysis was computed for the 12 variables assessed together to summarize the differential impacts of temperature on isolate IE and LP: IE at 5, 10, 15, 20 °C and LP at cold and warm regimes on varieties Victo and Cartago. R v. 3.1.2 (R Core Team) was used for all statistical analyses. If appropriate, initial full models were simplified by sequential removal of nonsignificant factors, starting with higher order interactions.

Infection efficiency modelling as a function of climate scenarios

A continuous model that predicted the effect of temperature and leaf wetness duration on IE was chosen. Magarey's well-known threshold-based model (Magarey *et al.*, 2005), designed to forecast pathogen development, was not used as it integrated temperature and leaf dew duration on both latency and infection phases as a whole. Rather, the model developed by de Vallavieille-Pope *et al.* (1995) was used, which estimated IE specifically as the product of maximal infection ($I_{\max}(T)$), and the relative Richards function of wetness duration with temperature-dependent parameters. $I_{\max}(T)$ is given by a beta function using five isolate-dependent parameters:

$$I_{\max}(T) = I_{\max} p \left[\frac{(T - T_{\min}) / (T_{\max} - T_{\min})}{(T_{\max} - T) / (T_{\max} - T_{\min})} \right]^n$$

where I_{\max} is the estimated maximal infection efficiency, T_{\max} and T_{\min} are the maximum and minimum temperatures for infection, respectively, n and m are shape parameters of the beta function, and $p = (n + m)^{n+m} / (n^n \cdot m^m)$ is directly derived from m and n values.

The following steps were followed to limit the fitted parameters; the experimentations were conducted under five temperatures, allowing no more than five fitted parameters. According to the literature on yellow rust general behaviour and in order to help the model to converge, IE data were forced to zero at 0 °C. At first, the five parameters were estimated altogether to fit the data; T_{\min} value was found close to zero with little variability among isolates, so that T_{\min} was further set at 0 °C. Then, as T_{\max} was the least variable of the four other parameters, it was set at 23 °C as it did not lead to variation on the quality of the fits. Finally, I_{\max} , n and m were the three parameters that characterized each isolate response to temperature (Table S1) and showed a coefficient of variation of 11, 22–24 and 24–30%, respectively. Correlations between observed and adjusted data were always significant and ranged between 0.66 and 0.86 (RRMSE ranging from 7% to 18%). The same function of dew duration was used for all isolates as defined in de Vallavieille-Pope *et al.* (2002). Thus, IE variations between isolates in future climate scenarios reflect only the differences in $I_{\max}(T)$ response to temperature. Optimal temperature (T_{opt}) was estimated per isolate and variety (Table S1): it varied between 14 and 17 °C and showed little variability (CV around 5%). As IE response to temperature between isolates varied more with I_{\max} , m and n parameters than with cardinal

temperatures T_{\min} , T_{\max} or T_{opt} , only the first three were used to simulate and disentangle isolate thermal behaviours under future climate scenarios.

To simulate the impact of climate change on IE of each Pst isolate, recent past (1971–2000), near future (2021–2050) and far (2071–2100) future climatic conditions were simulated using the French global climate model, ARPEGE, which is well adapted to the current European climate (Déqué *et al.*, 2005). The radiation transfer forcing in the model corresponds to greenhouse gas emission scenario A1B (Déqué *et al.*, 2005), a well-balanced average scenario corresponding to atmospheric concentrations of 541 ppm CO₂ by 2046–2065 increasing to 674 ppm by 2081–2100. The quantile–quantile statistical down-scaling method (Déqué, 2007) was applied to a northern temperate region (Versailles, 48°47'N 2°07'E) and a southern Mediterranean region (Avignon, 43°56'N 4°48'E) in France in order to assess climate change in two contrasted climatic zones. As climate models usually provide an estimate of future daily variables (temperature (T), relative humidity (RH) and rainfall), hourly values of T and leaf wetness duration (LWD) were generated from these daily climatic variables (Roche *et al.*, 2008; Launay *et al.*, 2014). Daily precipitation amounts were disaggregated into hourly values using a statistical approach reported by Allard & Bourotte (2015). Relative humidity and precipitation estimated for an hourly time step were then used as inputs of the LWD model designed by Lhomme & Jimenez (1992).

The model gave a predicted daily IE (%) value for each isolate on each variety over the three 30-year periods, allowing calculation of a mean simulated monthly IE. It allows simulation of a mean annual IE over the crop cycle (October to July inclusive) or a monthly IE to account for temporal evolutions in temperature and dew duration. An overall regression analysis between predicted IE in recent past and near or far future periods was used to analyse whether some isolates would benefit from climate change better than others. Therefore, a slope significantly greater than 1 indicates that the isolates with the highest IE in the recent past would have the highest IE increase in the future. In contrast, slopes significantly less than 1 indicate that the isolates with the highest IE in the recent past would have the lowest IE increase in the future. Finally, a slope equal to 1 with either a positive or a negative intercept shows a similar increase or decrease of IE for all isolates in the future.

Results

Infection efficiency

No infection was observed on leaves of either wheat variety after germination and penetration period at 23 °C. Analysis of variance for IE experiments indicated that all main effects (isolate, repetition and variety) were significant ($P < 10^{-4}$) for each dew period temperature of 5, 10 and 15 °C (Table 2). Generally, IE on Cartago was higher than on Victo. The reference isolate for a warm climate, S2, was the most efficient isolate, with a mean IE of 19.5% on all varieties and temperatures tested. Among the five temperatures tested under optimal dew duration, 10 °C showed the highest IE, ranging from 26% (isolate W8) to 38% (reference isolate S2) on Cartago, and from 13% (isolate W1) to 24% (isolate S2) on Victo. At 20°C, IE was extremely low. In fact, the Warrior isolate W9 was the least infective isolate at this

Table 2 Variance component analysis of infection efficiency of 16 *Puccinia striiformis* f. sp. *tritici* isolates according to the isolate (I) and the variety (Var) at three temperatures (5, 10 and 15 °C) and through two experimental repetitions (Rep).

Source	d.f.	Type I SS	Mean square	F-value	Pr > F
5 °C					
I	15	0.1560	0.0103	4.08	<10 ⁻⁴
Var	1	0.2070	0.2070	81.29	<10 ⁻⁴
Rep	1	0.2960	0.2960	116.49	<10 ⁻⁴
I × Var	15	0.0810	0.0054	2.12	0.0104
I × Rep	15	0.2790	0.0186	7.32	<10 ⁻⁴
Var × Rep	1	0.0194	0.0195	7.66	0.0061
Residuals	207	0.5270	0.0025		
10 °C					
I	15	0.2320	0.0155	3.72	<10 ⁻⁴
Var	1	2.0270	2.0270	486.79	<10 ⁻⁴
Rep	1	0.0304	0.0304	7.30	0.0075
I × Var	15	0.0818	0.0055	1.31	0.1987
I × Rep	15	0.6217	0.0414	9.96	<10 ⁻⁴
Var × Rep	1	0.0236	0.0236	5.67	0.0182
Residuals	207	0.8620	0.0042		
15 °C					
I	15	0.3474	0.0231	5.31	<10 ⁻⁴
Var	1	0.8084	0.8084	185.29	<10 ⁻⁴
Rep	1	0.0505	0.0505	11.58	0.0008
I × Var	15	0.1235	0.0082	1.89	0.0260
I × Rep	15	0.2187	0.0146	3.34	<10 ⁻⁴
Var × Rep	1	0.0612	0.0612	14.03	0.0002
Residuals	206	0.9031	0.0044		

Infection efficiency data were transformed into arcsin (square-root).

temperature, with IE < 0.05% on Cartago and zero on Victo.

Infection efficiencies assessed at different temperatures (5, 15 and 20 °C) were compared to IEs assessed at the intermediate temperature of 10 °C. Isolates with different thermal behaviours on both varieties were identified (Fig. 1). On Cartago at 5 °C, IE was almost half that observed at 10 °C. The reference isolate S2 yielded the highest IE and stood out from the other isolates, with an IE of 25% at 5 °C and 38% at 10 °C. Even though the same trends were observed for Victo, isolates had closer and lower IE means, i.e. maximum IE at 10 °C for S2 was 24%. On the other hand, the northern cold reference isolates (N1 and N2) showed an intermediate IE at 5 and 10 °C on both varieties. Intermediate IEs were found for PstS2 invasive isolates (P1–P3), averaging 14% and 18% at 5 °C and 17% and 32% at 10 °C for Victo and Cartago, respectively. In contrast, IE among the Warrior isolates varied at cold temperatures. A significant interaction between isolate and variety in IE response to temperature was found ($P = 0.01$; Table 2). The W5 and W9 isolates had approximately the same high IE (c. 20%) at 5 and 10 °C on Victo only, while W5 was the least infectious at 5 °C (on average 15%). At 15 °C the most efficient isolates were W9 (IE = 19.5%) on Cartago and S1 (IE = 15%) followed

by W9 (IE = 11.5%) on Victo. Furthermore, the other Warrior and PstS2 isolates showed intermediate IEs averaging 5.8% ($\pm 1.3\%$) on Victo and 13% ($\pm 2.4\%$) on Cartago. At 20 °C, IE was low compared to 10 °C, but discriminated isolates into groups, especially on Cartago.

Due to the very low rates of infection at 20 °C, the probability of infection (P_i) was estimated for each isolate (Table 3). Overall, the P_i s on Victo (0–0.4) were lower than on Cartago (0.1–0.9). The isolate W9 was the least efficient on both varieties at this temperature. On Victo, the P_i s of isolates W3 and W9 were significantly lower than most of the other Warrior isolates and the southern references S1 and S2. On Cartago, most isolates presented a P_i significantly higher than W9, except isolates W3, W7 and N2. At 20 °C on Cartago, S1, S2 and the PstS2 isolate P3 had the highest P_i , whilst on Victo, S1, S2, W6 and W8 had the highest P_i .

Latent period

The shorter the LP, the more aggressive the isolates were at a given temperature regime. Overall, LP was shorter for the warm post-inoculation temperature regime (from 185 to 222 hpi) than for the cold temperature regime (from 244 to 312 hpi). LP was also shorter on Victo (from 185 to 306 hpi) than on Cartago (from 186 to 312 hpi; Fig. 2). Both isolate and variety showed significant effects ($P < 10^{-4}$) on LP. In addition, all two-way interactions were significant with the cold regime, while only the isolate × repetition interaction was significant with the warm regime (Table 4). As expected, the two cold reference isolates N1 and N2 had the longest LP in the warm regime (average of 217 hpi between the two varieties) and among the shortest LP in the cold regime (average of 259 hpi). By contrast, the warm reference isolates S1 and S2 showed a long LP in the cold regime (average of 293 hpi), whilst in the warm regime they had amongst the shortest LP of all isolates tested on both varieties (average of 186 hpi).

The PstS2 isolates P1–P3 presented an intermediate to short LP on both varieties (on average 260 and 191.7 hpi in the cold and warm regime, respectively). Under the warm regime, P1 on both varieties and P2 and P3 on variety Victo had as short an LP as the reference isolates S1 and S2 (around 185 hpi on both varieties). Furthermore, the Warrior isolates displayed a relatively long to intermediate LP on both varieties and under the two temperature regimes (averaging 269.5 and 201.5 hpi under cold and warm regimes, respectively). The two isolates from triticale (W5 and W9) and one isolate from wheat (W7) presented a unique thermal response. W7 and W5 had short and long LP under cold and warm regimes on Cartago, respectively. On Victo, W5 showed the longest LP of the Warrior isolates under the warm regime, but amongst the shortest under the cold regime. W9 had a long LP under the cold regime on both varieties; under the warm regime it showed a long LP on Victo but amongst the shortest LP of all Warrior isolates on Cartago.

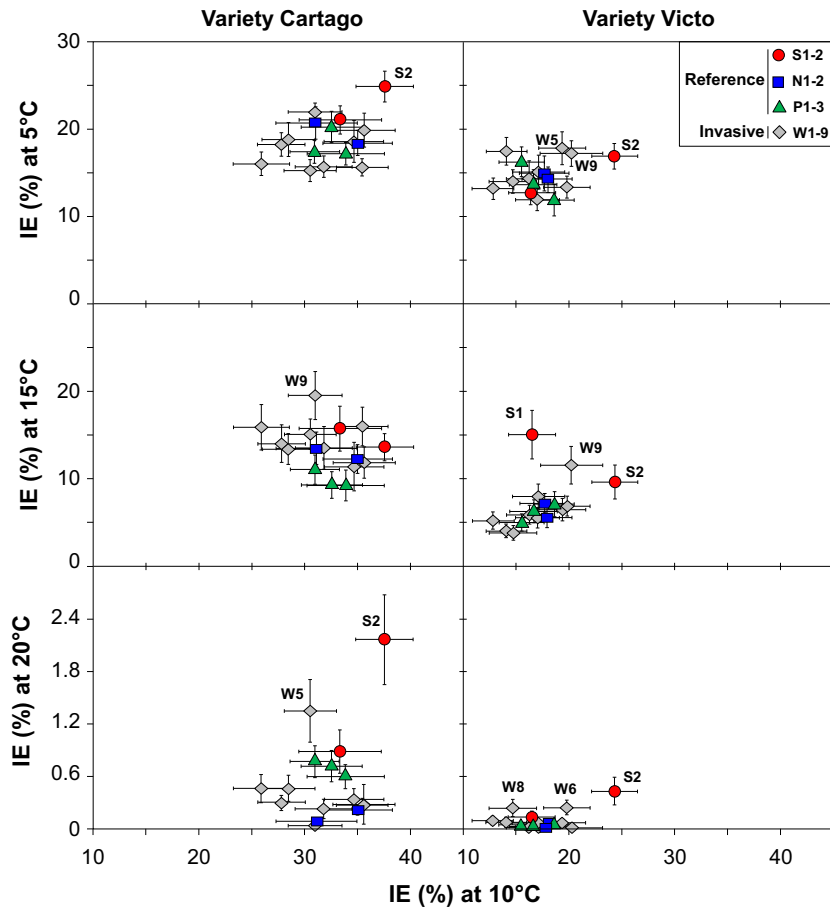


Figure 1 Infection efficiency (IE) of 16 *Puccinia striiformis* f. sp. *tritici* isolates on two susceptible wheat varieties (Cartago and Victo) at cold (5 °C), intermediate (15 °C) and high temperatures (20 °C) compared to IE at an optimal temperature of 10 °C. Each mean value is presented with \bar{x} - and \bar{y} -standard errors.

Table 3 Probability of infection (P_i) at 20 °C of 16 *Puccinia striiformis* f. sp. *tritici* isolates on varieties Cartago and Victo.

Cartago							Victo									
Isolate ^a	P_i						Isolate	P_i								
W9	0.100	a ^b					W9	0	a							
W3	0.163	a	b				W3	0.012	a							
N2	0.238	a	b	c			N2	0.038	a	b						
W7	0.325	a	b	c	d		W7	0.038	a	b	c					
N1	0.438		b	c	d	e	P2	0.050	a	b	c					
W4	0.488		b	c	d	e	f	P1	0.050	a	b	c				
W2	0.488			c	d	e	f	N1	0.088	a	b	c	d			
W6	0.525				c	d	e	f	W2	0.088	a	b	c	d		
W1	0.538					d	e	f	P3	0.088	a	b	c	d		
W5	0.551						d	e	f	W5	0.112		b	c	d	
W8	0.584						d	e	f	W1	0.150		b	c	d	
P1	0.738							e	f	W4	0.150		b	c	d	
P2	0.763								f	S1	0.188		b	c	d	
S1	0.788									W8	0.325			c	d	
S2	0.800									S2	0.350				c	d
P3	0.875									W6	0.400					d

^aN1, N2, S1 and S2: reference isolates from the north and south of France, respectively; P1–3: PstS2 reference isolates; W1–9: Warrior isolates.

^ba–f: classification according to Newman–Keuls comparison at 5% significance level.

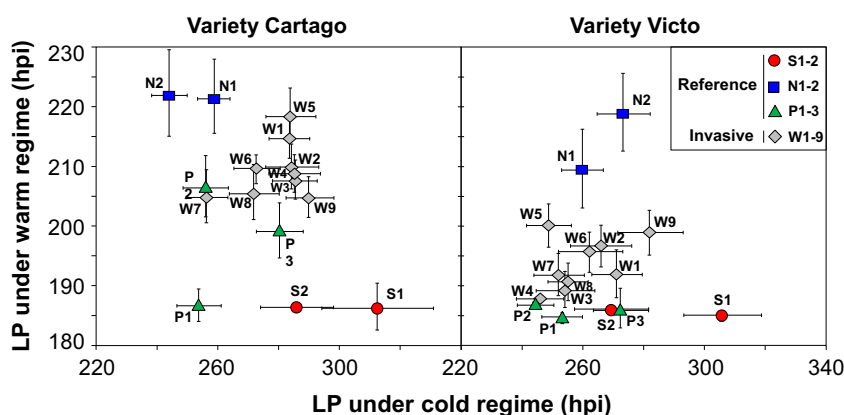


Figure 2 Latent period (LP) of 16 *Puccinia striiformis* f. sp. *tritici* isolates inoculated onto two susceptible wheat varieties (Cartago and Victo) and incubated under warm (16/25 °C) and cold (10/15 °C) temperature regimes. Each mean value is presented with x- and y-standard errors.

Table 4 Variance component analysis of latent period of 16 *Puccinia striiformis* f. sp. *tritici* isolates according to the isolate (I) and the variety (Var) under the two warm and cold temperature regimes and through two experimental repetitions (Rep).

Source	d.f.	Type I SS	Mean square	F-value	Pr > F
10/15 °C					
I	15	51424.2	3428.3	10.7	<10 ⁻⁴
Var	1	7128.6	7128.6	22.2	<10 ⁻⁴
Rep	1	2441.0	2441.0	7.6	0.0063
I × Var	15	16679.8	1112.0	3.5	<10 ⁻⁴
I × Rep	15	20273.0	1351.5	4.2	<10 ⁻⁴
Var × Rep	1	68.2	68.2	0.2	0.6452
Residuals	207	66349.9	320.5		
16/25 °C					
I	15	31909.6	2127.3	23.2	<10 ⁻⁴
Var	1	9962.5	9962.5	108.6	<10 ⁻⁴
Rep	1	35.9	35.9	0.4	0.0063
I × Var	15	1780.2	118.7	1.3	0.2086
I × Rep	15	3051.3	203.4	2.2	0.0069
Var × Rep	1	27.9	27.9	0.3	0.5823
Residuals	206	18904.9	91.8		

Temperature profiles of the isolates according to their IE and LP

Thermal profiles of all 16 Pst isolates were achieved using principal components analysis (PCA) on the two varieties using IE and LP together under different thermal regimes. The two-first components of the PCA accounted for 51.4% of the total variation (Table 5). The variable IE at 5 °C for Victo and IE at 10 °C for Cartago were the least represented in this factorial plan. The first PCA axis (PC1) explained 34.2% of the variation; all IE variables contributed almost equally to PC1, while LP under the warm regime was negatively correlated with PC1. Consequently, PC1 separated isolates combining consistently high IE at all temperatures and short LP in the warm regime from those having relatively low IE at all temperatures. The second component (PC2) accounted for 17.2% of the total variation and was less correlated with LP and IE. It separated noninfective isolates on Cartago and Victo at 10 and 20 °C

Table 5 Eigenvectors of the two principal components axes (PC1 and PC2) for the 12 variables assessed (infection efficiency, IE, at 5, 10, 15 and 20 °C and latent period, LP, under cold and warm temperature regimes on two susceptible varieties, Victo and Cartago) and their contribution to percentage of variance.

Variable	PC1	PC2
IE 5 Cartago	0.72	0.20
IE 10 Cartago	0.41	-0.22
IE 15 Cartago	0.32	0.68
IE 20 Cartago	0.68	-0.47
LP Cold Cartago	0.65	0.23
LP Warm Cartago	-0.71	0.47
IE 5 Victo	0.28	0.30
IE 10 Victo	0.60	-0.04
IE 15 Victo	0.76	0.35
IE 20 Victo	0.62	-0.25
LP Cold Victo	0.59	0.54
LP Warm Victo	-0.39	0.67
Eigenvalue	4.10	2.06
Percentage of variance (%)	34.20	17.19

from those that were efficient at those temperatures. For both varieties, this analysis showed that high IE at 20 °C was negatively correlated with long LP in the warm regime (Table 5). Low IE at 5 °C was related to a long LP in the cold regime (Fig. 3).

The PC1 and PC2 components divided the 16 Pst isolates into five temperature profiles (Fig. 3). The warm reference isolates S1 and S2 grouped together, with S2 being more efficient than S1 at all temperatures. The northern reference isolates N1 and N2 presented a similar temperature profile on both varieties (low IE and long LP under warm temperatures), with a stronger impact of N1 than N2 at 10 °C. Isolates P1–P3 had low to moderate IE and intermediate LP in cold and warm regimes. Most of the Warrior isolates (except W9 and to a lesser extent W7) were grouped together in the central area of the PC1–PC2 plan, between the N1–N2 group and P1–P3 group. This Warrior isolate group presented an intermediate IE and LP compared to the extreme reference isolates. Isolate W9 stood out from the Warrior group and was closer to S1 with a higher infectivity on Cartago

Figure 3 Plot of 16 isolates of *Puccinia striiformis* f. sp. *tritici* projected onto the two first principal components (PC1 and PC2) and according to 12 variables (infection efficiency at 5, 10, 15 and 20 °C and latent period at cold and warm temperature regime) tested on two susceptible wheat varieties (Victo and Cartago). The significance of the axes is given in the corners of the graph: IE_{warm} and IE_{cold} indicate infection efficiency under warm (15, 20 °C) and cold (5, 10 °C) temperatures, respectively; LP_{warm} and LP_{cold} indicate latent period under warm and cold temperature regimes, respectively; + indicates high IE and short LP, - indicates low IE and long LP.

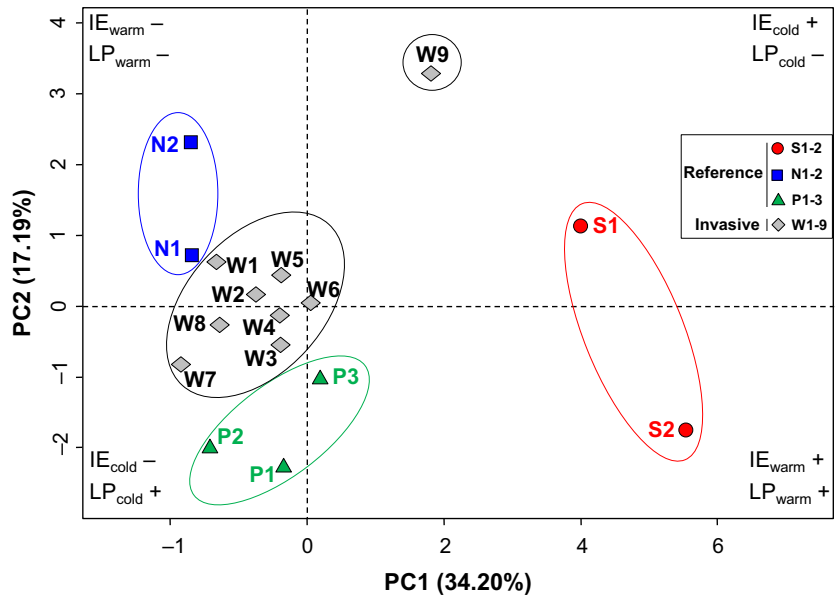
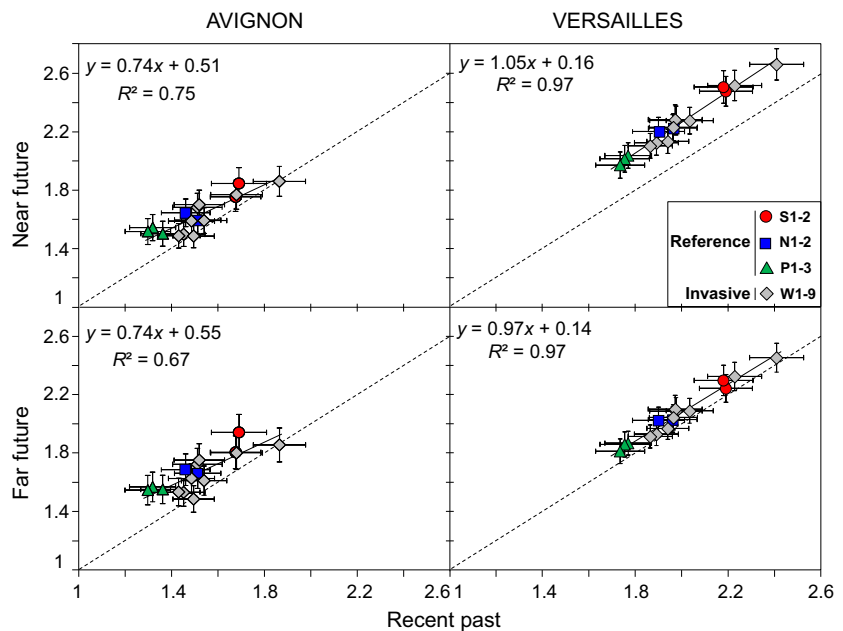


Figure 4 Prediction of a mean annual infection risk for 16 isolates of *Puccinia striiformis* f. sp. *tritici* on wheat variety Cartago at two locations (Avignon and Versailles, France) for three climate periods: recent past (1971–2000), near future (2021–2050) and far future (2071–2100). Each mean value is presented with x- and y-standard errors. Dashed line represents the 1:1 line.



than Victo, especially at 15 °C, and a long LP under a cold temperature regime.

Projections of IE in recent past, near future and far future scenarios for invasive isolates

Previous experimental data allowed the observed IE to be fitted to a thermal response curve for each isolate. These curves were then used to estimate IE of each isolate in the future. Overall, mean annual IEs were slightly higher in the near future (NF) and far future (FF) compared to the recent past (RP). Furthermore, median IE

values of the isolates in the future (NF and FF) were above recent past IE values (Fig. 4 for Cartago and Fig. S1 for Victo). However, intercepts were never found significantly different from zero ($P > 0.10$) and isolates remained similarly classified for annual IE, given that the slopes of IE from the recent past to the futures did not differ significantly ($P > 0.28$), for Versailles conditions. This annual IE increase in the future was slightly significant in Avignon, with slopes between recent past IE and future IE different from one in NF ($P < 0.05$) but not in FF ($P > 0.05$), while intercepts were always found significantly higher than zero ($P < 0.05$). Moreover, the

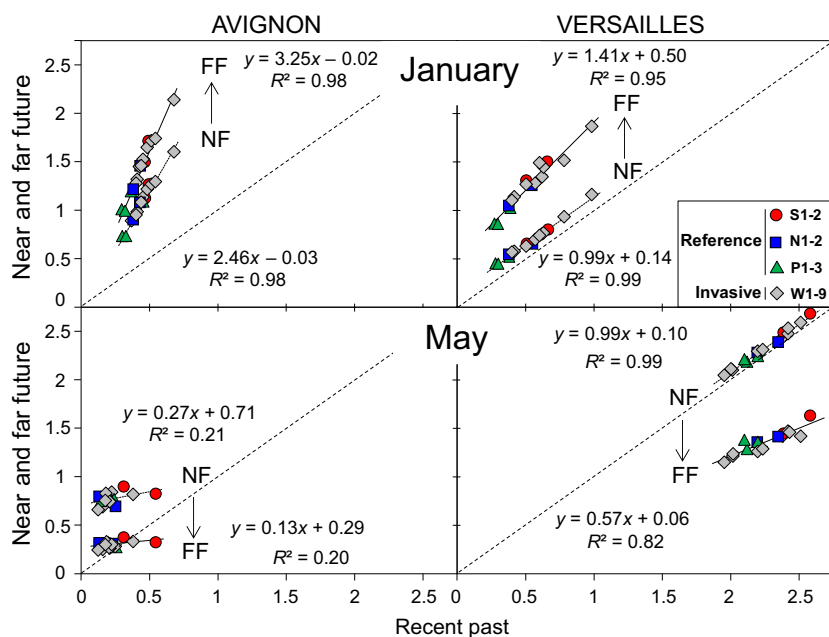


Figure 5 Regression of mean monthly *Puccinia striiformis* f. sp. *tritici* infection efficiencies from the recent past (1971–2000) to the near future (NF: 2021–2050) and the far future (FF: 2071–2100) in the southern French site, Avignon, and the northern site, Versailles, in the case of wheat variety Cartago in January and May. Dashed line represents the 1:1 line. Arrows indicate the global trend from NF to FF in each case.

increase in IE was not significantly higher in the NF than in the FF, with similar intercepts or slopes ($P > 0.05$). These data suggested that all Warrior isolates except one did not show a mean annual advantage in the future, as their IEs remained between those of northern and southern reference isolates, the latter having the highest IE. An exception was noticed for W9 that maintained higher IE values than southern reference isolates in the future. Despite responses to climate change being larger for Cartago than for Victo, the overall trends were conserved (Table S2).

As the annual IE averages mask monthly differences in the responses to climate change, IEs were estimated for January and May, characterizing the beginning and end of the epidemics. Monthly regressions of IE in the NF and FF to IE in the RP were shown for Cartago (Fig. 5) and Victo (Fig. S2). An increase of IE was observed in January with climate change, suggesting earlier epidemics in the future, with more outbreaks in southern regions (Fig. 5). In fact, the probability of reaching the 1% threshold IE every day increases in January by 7% and 4% in the NF and by 3% and 14% in the FF, for Avignon and Versailles, respectively. This increase is of the same order of magnitude in December (data not shown). This result relies on the relative increase in temperatures in January (T_{dew} increased around $+2$ °C between RP and FF), closer to optimal temperatures for IE, while dew durations do not limit infection (higher than 9 h in all cases; Fig. S3). A differential response of isolates was observed in Avignon. Isolates adapted to higher temperatures, like the southern reference isolates and some Warrior isolates, notably W9 and to a lesser extent W8, benefited most from increased temperatures in the future.

Conversely in May, IEs were found to stagnate or increase in NF compared to RP, and decreased in FF, for

half of the isolates in Avignon and all isolates in Versailles (Fig. 5). The probability to reach the threshold of 1% IE every day decreased by around 3% in May in FF. This trend was reinforced in June (data not shown). IE values were at least twice as low in Avignon than in Versailles. In Avignon, the range of IEs was reduced in the future scenario. This was because of dew durations lower than 6 h that limited the infection process. The slight increase in temperature by 1.5 °C during the dew duration benefits infection in the NF, while the decrease in dew duration to 1 and 3.5 h, in Avignon and Versailles respectively, limits infection in FF. In Versailles, temperature and dew duration did not vary much between RP and NF, which resulted in similar IE values. Conversely, temperatures remained near the optimum while dew duration decreased by approximately 20% in FF, resulting in the decrease of IE values.

Discussion

This study investigated the thermal aptitude of Warrior isolates that recently invaded Europe and compared them to northern and southern French isolates present locally for decades and to PstS2 isolates from worldwide origins. The goal was to determine the extent to which the thermal aptitude could explain the development of these exotic strains in temperate and Mediterranean areas and to simulate their IEs in future climate scenarios.

Among the tested temperatures, no infection was observed at 23 °C. Rapilly (1979) reported that 22 °C was the highest temperature for spore penetration, but once in the plant, the pathogen could tolerate higher temperature. Furthermore, Dennis (1987) agreed with Rapilly (1979) that optimum, maximum and minimum temperatures were 7–10 °C, 18 °C and 0 °C,

respectively. More recently, Mboup *et al.* (2012) confirmed that incubation at 25 °C under nonlimiting wetness conditions caused a hypersensitive reaction leading to total host resistance. Under high level of light before inoculation, maximal IE was observed at 14.5 °C for a northwestern isolate, whereas 8 °C was the optimal temperature under darkness before inoculation (de Vallavieille-Pope *et al.*, 2002).

The results here confirm the specialist thermal behaviour of the reference isolates as shown previously for local French reference isolates (Mboup *et al.*, 2012). The southern French isolates (S1 and S2) could infect wheat at 20 °C with short LP under a warm regime. The northern French isolates (N1 and N2) were not able to colonize the host at such warm temperatures; only rare infections occurred after a long LP. These isolates showed higher performance at lower temperature in agreement with their adaptation to temperate zones in northern France. PstS2 isolates that are adapted to warm climates (Milus *et al.*, 2009) and belong to the genetic group of the Middle East and Mediterranean area (Walter *et al.*, 2016), had an intermediate thermal response at 5, 10 and 15 °C, and a short LP on both varieties and temperature regimes. PstS2 isolates also had the highest IEs of all the isolates tested at 20 °C on Cartago. This thermal adaptation trait can lead to dominance of PstS1/PstS2 strains in warmer geographic areas, as recently found in new areas for wheat yellow rust, with PstS1 in the southern United States (Milus *et al.*, 2009) and western Australia (Wellings, 2011; Loladze *et al.*, 2014), and PstS2 in southern France (de Vallavieille-Pope *et al.*, 2012), the Mediterranean area (Bahri *et al.*, 2009) and Asia (Hovmøller *et al.*, 2011). However, the PstS2 isolates tested here under warm regime conditions did not perform as well as the S1 and S2 isolates (PstS3), previously found in the Mediterranean area. Furthermore, Loladze *et al.* (2014) found that thermal aptitude alone could not explain the development of the PstS1 clonal lineage in Australia since 2002. Australian PstS1 isolates did not perform better than pre-2002 isolates under the warm regime. It is important to note that both virulence and thermal aptitude are under selection, leading to the development of different clonal lineages in specific areas.

In contrast to the reference isolates, the Warrior isolates behaved as generalists for IE and LP on both wheat varieties, with an efficient infection aptitude at 10 and 15 °C, and a reduced infectivity at 20 and 5 °C. In contrast to the Warrior isolates found on bread wheat, isolates W5 and W9 sampled from triticale showed high infectivity at most temperatures, suggesting that this trait could be associated with host specificity. Furthermore, the LP of Warrior isolates was intermediate between that of the two northern and southern reference isolates. Differences were observed in IE and LP among the Warrior isolates. Several recent studies demonstrated a significant molecular diversity of exotic races, such as Warrior and Kranich, compared to European and pre-existing clonal populations (Hubbard *et al.*, 2015; Hovmøller *et al.*, 2016; Walter *et al.*, 2016). Given that sexuality was

observed recently under controlled conditions in Pst (Jin *et al.*, 2010) and in particular with a Warrior isolate (Rodriguez-Algaba *et al.*, 2014), genetic recombination could be a source of this phenotypic variability. For instance, possible aggressive variants in a Warrior strain could be selected, as some differences between offsprings issued from selfing of one isolate were observed for LP (Sørensen *et al.*, 2015). Diversity in thermal responses was shown previously in several pathosystems under controlled conditions between and within clonal lineages. Some Pst isolates from two clonal lineages, PstS1 in the US (Milus *et al.*, 2009) and PstS3 in France (Mboup *et al.*, 2012), showed higher levels of aggressiveness at high temperatures than pre-2000 North American isolates and northwestern European isolates, respectively. Local thermal adaptation was shown with *Zymoseptoria tritici* isolates from two warm zones which performed better for *in vitro* growth rate under high temperatures than isolates from two cool locations (Zhan & McDonald, 2011). Local thermal adaptation was also observed for *Phytophthora infestans* isolates collected in different climatic zones (Mariette *et al.*, 2016a), even though variability was observed among clonal lineages living in sympatry in western Europe.

Interactions between variety and isolate depended on the temperature, but IE and LP covaried mainly positively. A variety effect was detected for IE and LP at all temperatures tested. For IE and LP, Cartago separated the isolates better than Victo, especially at warm temperatures. Northern isolates had the longest LP while southern isolates and P1 (PstS2) had the shortest. Differences in aggressiveness among isolates have been reported to be greatest under nonoptimal conditions, as exemplified on LP for *Puccinia triticina* and Pst isolates (Eversmeyer *et al.*, 1980; Johnson, 1980; Milus *et al.*, 2006). Furthermore, an interaction between variety and isolate was observed for LP at cold temperature regimes and for IE at 5 and 15 °C. Significant interactions between two Pst isolates, one northwestern and one Warrior isolate, and quantitative trait for resistance (QTL) were also observed for lesion length and LP (Sørensen *et al.*, 2014). An interaction between temperature regime, isolate and variety was also noticed in this study for IE and LP, i.e. the PstS2 isolates were distinguished for LP under the warm regime on Cartago, but were similar on Victo. Isolate × temperature interaction was previously described for spore production rate of two *P. triticina* isolates, which was identical at 2–18 °C but differed at 10–30 °C (Milus & Line, 1980).

Positive correlation and trade-off between aggressiveness variables have previously been reported for fungal pathogens (Pariaud *et al.*, 2009). In the current study, positive correlation was observed between IE at 10 and 20 °C and LP under a warm regime, especially for N2 and S2. Furthermore, a trade-off between IE at 5 and 15 °C and LP under a cool regime for some Warrior and PstS2 isolates and S1 was observed. For Warrior isolates (W4 and W7) or PstS2 isolates (P1–P3), intermediate IE at all tested temperatures was compensated for by a

relatively short LP under both temperature regimes. This increased the chances of plant colonization by the pathogen.

Studying the effect of temperature on pathogen fitness represents a way to predict the ecological risk of increase in disease development under climate change (Zhan & McDonald, 2011; Helfer, 2014). Under global warming conditions (Garrett *et al.*, 2011), pathogens are expected to withstand new thermal fluctuations. Thus, generalists such as the Warrior isolates would take advantage over the specialists adapted to only warm or cool conditions such as southern and northern Pst isolates, respectively. Predicting the IE of isolates under different future climate scenarios did not show this trend. No clear advantage of the Warrior isolates was observed in terms of mean annual IE response to temperature in the future climate, regardless of the wheat variety and the period; they mainly remained between those of the southern and northern references, with the southern reference isolates performing better under actual and future climate. The simulation of mean annual IE under future climate conditions did not lead to the prediction of the future dominance of invasive strains. Nonetheless, infra-annual IE patterns were examined. It was found that infection would begin earlier in winter in the future, benefiting from higher temperatures at nonlimiting dew durations, and the ranking between isolates was conserved. It was also found that infection would end earlier in spring, when temperatures become suboptimal and dew duration too short for infection. These trends were previously reported for a range of foliar pathogens (Launay *et al.*, 2014). However, even if future climate favours some isolates due to their IE response to temperature, no clear Warrior isolate outliers were observed in the present study.

Limits to strain-specific IE predictions with climate change may be noticed. First, the parameterization of reaction norms of IE to temperature could be improved between 0 and 5 °C, as local thermal adaptation may also result in a switch of T_{\min} , leading to earlier epidemics. Note, nevertheless, that IE fitting led to values in accordance with expected biological ranges: T_{\max} mainly ranged from 18 to 24 °C as previously described (Rapilly, 1979; Mboup *et al.*, 2012), with few outliers. Finally, LP was not taken into account in the present modelling study, as experimental data with only two temperature regimes were not sufficient to fit LP response function to temperature per isolate. The thermal response of multiple traits should be addressed to account for trade-offs between traits and predict overall aggressiveness in the future. However, Pariaud *et al.* (2009) and Mboup *et al.* (2012) found that aggressiveness traits covary, suggesting that one trait may be sufficient to infer aggressiveness. This covariation of aggressiveness traits was also recently described for *P. infestans* (Mariette *et al.*, 2016a) under a range of temperatures. If the present experimental and modelling results follow the same trend, thermal aptitude would not be related to invasive potential of Pst strains.

This is consistent with recent findings that dominant invasive clones of *P. infestans* isolates exhibit low or

moderate aggressiveness relative to local populations. Invasive behaviour was not directly linked to increased aggressiveness, at least for the measured traits (Mariette *et al.*, 2016b). Moreover, the most invasive strain combined average traits of aggressiveness. Surprisingly, in the case of wheat yellow rust, PstS2 strains always showed low IE values under NF and FF climate; their invasive advantage may be better linked to their short LP in cold and warm conditions, as observed in the present study. Mariette *et al.* (2016b) hypothesized that this opposition between invasive behaviour and aggressiveness may also result from a trade-off between survival and multiplication phases that occur successively each year.

To conclude, the reference southern isolates tested in the current study performed the best under actual and future climate scenarios using a simple analytical IE model. However, those isolates lacked several virulences to enable them to infect northwestern European wheat varieties. Therefore, Warrior isolates with intermediate temperature aptitude and carrying as many virulence factors as northwestern European races, appear to be good competitors for facing the specialist strains adapted to either warm or cool conditions.

Acknowledgements

The authors are grateful to Laurent Gérard for his technical assistance in cultivating the plants in the greenhouse, to Fabien Jankowiak for data analysis and to Ron Walcott for reviewing the manuscript. This study received financial support from KBBE 219262, INRA ACCAF Metaprogramme CLIF and 2014-16 PHC-Utique (14G 0909) projects. The study was also supported by Innovation Fond Denmark, Ministry of Higher Education and Science, RUSTFIGHT (grant number 11-116241).

References

- Ali S, Gautier A, Leconte M, Enjalbert J, de Vallavieille-Pope C, 2011. A rapid genotyping method for an obligate fungal pathogen, *Puccinia striiformis* f. sp. *tritici*, based on DNA extraction from infected leaf and multiplex PCR genotyping. *BMC Research Notes* 4, 240.
- Ali S, Gladieux P, Leconte M *et al.*, 2014. Origin, migration routes and worldwide population genetic structure of the wheat yellow rust pathogen *Puccinia striiformis* f. sp. *tritici*. *PLoS Pathogens* 10, e1003903.
- Allard D, Bourotte M, 2015. Disaggregating daily precipitations into hourly values with a transformed censored latent Gaussian process. *Stochastic Environmental Research and Risk Assessment* 29, 453–62.
- Bahri B, Leconte M, Ouffroukh A, de Vallavieille-Pope C, Enjalbert J, 2009. Geographic limits of a clonal population of wheat yellow rust in the Mediterranean region. *Molecular Ecology* 18, 4165–79.
- Bebber DP, 2015. Range-expanding pests and pathogens in a warming world. *Annual Review of Phytopathology* 53, 335–56.
- Bernard F, Sache I, Suffert F, Chelle M, 2013. The development of a foliar fungal pathogen does react to leaf temperature! *New Phytologist* 198, 232–40.
- Brown JKM, Hovmöller MS, 2002. Aerial dispersal of pathogens on the global and continental scales and its impact on plant disease. *Science* 297, 537–41.
- Chen XM, 2005. Epidemiology and control of stripe rust [*Puccinia striiformis* f. sp. *tritici*] on wheat. *Canadian Journal of Plant Pathology* 27, 314–37.

- Chen W, Wellings C, Chen X, Kang Z, Liu T, 2014. Wheat stripe yellow rust caused by *Puccinia striiformis* f. sp. *tritici*. *Molecular Plant Pathology* 15, 433–46.
- Dennis JL, 1987. Temperature and wet-period conditions for infection by *Puccinia striiformis* f. sp. *tritici* race 104E137A+. *Transactions of the British Mycological Society* 88, 119–21.
- Déqué M, 2007. Frequency of precipitation and temperature extremes over France in an anthropogenic scenario: model results and statistical correction according to observed values. *Global and Planetary Change* 57, 16–26.
- Déqué M, Jones RG, Wild M *et al.*, 2005. Global high resolution versus Limited area model climate change projections over Europe: quantifying confidence level from PRUDENCE results. *Climate Dynamic* 25, 653–70.
- Eversmeyer MG, Kramer CL, Browder LE, 1980. Effect of temperature and host: parasite combination on the latent period of *Puccinia recondita* in seedling wheat plants. *Phytopathology* 70, 938–41.
- Garrett KA, Forbes GA, Savary S *et al.*, 2011. Complexity in climate-change impacts: an analytical framework for effects mediated by plant disease. *Plant Pathology* 60, 15–30.
- Helfer S, 2014. Rust fungi and global change. *New Phytologist* 201, 770–80.
- Hovmöller MS, Sørensen CK, Walter S, Justesen AF, 2011. Diversity of *Puccinia striiformis* on cereals and grasses. *Annual Review of Phytopathology* 49, 197–217.
- Hovmöller MS, Walter S, Bayles RA *et al.*, 2016. Replacement of the European wheat yellow rust population by new races from the centre of diversity in the near-Himalayan region. *Plant Pathology* 65, 402–11.
- Hubbard A, Lewis C, Yoshida K *et al.*, 2015. Field pathogenomics reveals the emergence of a diverse wheat yellow rust population. *Genome Biology* 16, 23.
- Jin Y, Szabo LJ, Carson M, 2010. Century-old mystery of *Puccinia striiformis* life history solved with the identification of *Berberis* as an alternate host. *Phytopathology* 100, 432–5.
- Johnson DA, 1980. Effect of low temperature on the latent period of slow and fast rusting winter wheat genotypes. *Plant Disease* 64, 1006–8.
- Johnson R, Stubbs RW, Fuchs E, Chamberlain NH, 1972. Nomenclature for physiologic races of *Puccinia striiformis* infecting wheat. *Transactions of the British Mycological Society* 58, 475–80.
- Launay M, Caubel J, Bourgeois G *et al.*, 2014. Climatic indicators for crop infection risk: application to climate change impacts on five major foliar fungal diseases in northern France. *Agriculture, Ecosystems and Environment* 197, 147–58.
- Lhomme JP, Jimenez F, 1992. Estimating dew duration on banana and plantain leaves from standard meteorological observations. *Agricultural and Forest Meteorology* 62, 263–74.
- Loladze A, Druml T, Wellings CR, 2014. Temperature adaptation in Australasian populations of *Puccinia striiformis* f. sp. *tritici*. *Plant Pathology* 63, 572–80.
- Magarey RD, Sutton TB, Thayer CL, 2005. A simple generic infection model for foliar fungal plant pathogens. *Phytopathology* 95, 92–100.
- Mariette N, Androdias A, Mabon R *et al.*, 2016a. Local adaptation to temperature in populations and clonal lineages of the Irish potato famine pathogen *Phytophthora infestans*. *Ecology and Evolution* 6, 6320–31.
- Mariette N, Mabon R, Corbière R *et al.*, 2016b. Phenotypic and genotypic changes in French populations of *Phytophthora infestans*: are invasive clones the most aggressive? *Plant Pathology* 65, 577–86.
- Mboup M, Bahri B, Leconte M, de Vallavieille-Pope C, Kaltz O, Enjalbert J, 2012. Genetic structure and local adaptation of European wheat yellow rust populations: the role of temperature-specific adaptation. *Evolutionary Applications* 5, 341–52.
- McNeal FH, Konzak CF, Smith EP, Tate WS, Russel TS, 1971. A uniform system for recording and processing cereal research data. *USDA Agricultural Research Service Bulletin* 42, 34–121.
- Milus EA, Line RF, 1980. Characterization of resistance to leaf rust in Pacific Northwest wheat lines. *Phytopathology* 70, 167–72.
- Milus EA, Seyran E, McNew R, 2006. Aggressiveness of *Puccinia striiformis* f. sp. *tritici* isolates in the south-central United States. *Plant Disease* 90, 847–52.
- Milus EA, Kristensen K, Hovmöller MS, 2009. Evidence for increased aggressiveness in a recent widespread strain of *Puccinia striiformis* f. sp. *tritici* causing stripe rust of wheat. *Phytopathology* 99, 89–94.
- Paillard S, Trotoux-Verplanck G, Perretant M-R *et al.*, 2012. Durable resistance to stripe rust is due to three specific resistance genes in French bread wheat cultivar Apache. *Theoretical and Applied Genetics* 125, 955–65.
- Pariaud B, Ravigné V, Halkett F, Goyeau H, Carlier J, Lannou C, 2009. Aggressiveness and its role in the adaptation of plant pathogens. *Plant Pathology* 58, 409–24.
- Rapilly F, 1979. Yellow rust epidemiology. *Annual Review of Phytopathology* 17, 59–73.
- Roche R, Bancal MO, Gagnaire N, Huber L, 2008. Potential impact of climate change on brown wheat rust: a preliminary study based on biophysical modelling of infection events and plant–pathogen interactions. *Aspects of Applied Biology* 88, 135–42.
- Rodriguez-Algaba J, Walter S, Sørensen CK, Hovmöller MS, Justesen AF, 2014. Sexual structures and recombination of the wheat rust fungus *Puccinia striiformis* on *Berberis vulgaris*. *Fungal Genetics and Biology* 70, 77–85.
- Schwessinger B, 2016. Fundamental wheat stripe rust research in the 21st century. *New Phytologist* 213, 1625–31.
- Sørensen CK, Hovmöller MS, Leconte M, Dedryver F, de Vallavieille-Pope C, 2014. New races of *Puccinia striiformis* found in Europe reveal race specificity of long-term effective adult plant resistance in wheat. *Phytopathology* 104, 1042–51.
- Sørensen CK, Rodriguez-Algaba J, Justesen AF, Hovmöller MS, 2015. Segregation for aggressiveness in sexual offspring of the yellow rust pathogen *Puccinia striiformis*. In: *Borlaug Global Rust Initiative Technical Workshop, Sydney, Australia, 17–20 September 2015*. [https://www.globalrust.org/2015-plenary-abstracts#sorensen]. Accessed 29 January 2018.
- Sørensen CK, Thach T, Hovmöller MS, 2016. Evaluation of spray and point inoculation methods for the phenotyping of *Puccinia striiformis* on wheat. *Plant Disease* 100, 1064–70.
- Sutherst RW, Constable F, Finlay KJ, Harrington R, Luck J, Zalucki MP, 2011. Adapting to crop pest and pathogen risks under a changing climate. *Interdisciplinary Reviews: Climate Change* 2, 220–37.
- de Vallavieille-Pope C, Huber L, Leconte M, Goyeau H, 1995. Comparative effects of temperature and interrupted wet periods on germination, penetration, and infection of *Puccinia recondita* f. sp. *tritici* and *P. striiformis* on wheat seedlings. *Phytopathology* 85, 409–15.
- de Vallavieille-Pope C, Huber L, Leconte M, Bethenod O, 2002. Preinoculation effects of light quantity on wheat seedlings on infection efficiency of *Puccinia striiformis* and *P. triticina*. *Phytopathology* 92, 1308–14.
- de Vallavieille-Pope C, Ali S, Leconte M, Enjalbert J, Delos M, Rouzet J, 2012. Virulence dynamics and regional structuring of *Puccinia striiformis* f. sp. *tritici* in France between 1984 and 2009. *Plant Disease* 96, 131–40.
- Walter S, Ali S, Kemen E *et al.*, 2016. Molecular markers for tracking the origin and worldwide distribution of invasive strains of *Puccinia striiformis*. *Ecology and Evolution* 6, 2790–804.
- Wellings CR, 2011. Global status of stripe rust: a review of historical and current threats. *Euphytica* 179, 129–41.
- Zhan J, McDonald BA, 2011. Thermal adaptation in the fungal pathogen *Mycosphaerella graminicola*. *Molecular Ecology* 20, 1689–701.

Supporting Information

Additional Supporting Information may be found in the online version of this article at the publisher's web-site.

Figure S1. Prediction of a mean annual infection risk for 16 isolates of *Puccinia striiformis* f. sp. *tritici* on wheat variety Victo at two locations (Avignon and Versailles) for three climate periods: recent past (1971–2000), near future (2021–2050) and far future (2071–2100). Each mean value is presented with x - and y -standard errors. Dashed line represents the 1:1 line.

Figure S2. Regression of mean monthly *Puccinia striiformis* f. sp. *tritici* infection efficiency from the recent past (1971–2000) to the near future (NF: 2021–2050) and the far future (FF: 2071–2100) in the southern French site of Avignon, and the northern site of Versailles, for wheat variety Victo in January and May. Dashed line represents the 1:1 line. Arrows indicate the global trend from NF to FF in each case.

Figure S3. Mean monthly temperature during dew period ($T^{\circ}\text{dew}$, °C) and dew duration (h) estimated in recent past (RP), near future (NF) and far future (FF) in January and May at Avignon and Versailles, France, according to a warming climate scenario A1B from the Special Report on Emissions Scenarios (SRES). Boxplots show minimal (○) and maximal (●), median, first and third quartile values over the 30 years of each period (RP: 1971–2000; NF: 2021–2050; FF: 2071–2100).

Table S1. Isolate-specific infection efficiency (IE) parameters (I_{max} (%), m and n) characterizing IE response-curve to temperature and calculated temperatures from the fits for minimal temperature required to reach 5% of I_{max} ($T_{\text{min-5\%}I_{\text{max}}}$), optimal temperature (T_{opt}) and maximal temperature required to reach 5% of I_{max} ($T_{\text{max-5\%}I_{\text{max}}}$), for variety Cartago and variety Victo.

Table S2. Regression lines relating predicted monthly infection efficiency values of *Puccinia striiformis* f. sp. *tritici* isolates in recent past and either near or far future for two wheat varieties (Cartago and Victo) at a southern (Avignon) and a northern (Versailles) site in France.